Article

Assessing grass water use efficiency through smartphone imaging and ImageJ analysis

Aniyah X. Shen[1], Francesco Palomba[2], Wanqi Jia[1], Michelle A. Digman[2]
[1]University High School, Irvine, California
[2]University of California, Irvine, California

SUMMARY

Overwatering and underwatering grass are widespread issues with environmental and financial consequences. Current approaches to assessing grass water use efficiency (WUE) are inaccessible to the public. We developed an accessible method to assess grass WUE: combining smartphone imaging with open access color unmixing analysis. Images were converted from the RGB color space to the CIELAB color space using ImageJ—an open-access, user-friendly software—to correct for uneven lighting without compromising image detail. We obtained parameters $a*$ (unmixes green-to-red vector) and $b*$ (unmixes blue-to-yellow vector). We hypothesized that WUE can be accurately determined from grass color and growth, which can be analyzed using CIELAB color unmixing. We tested how nine watering levels (100–900 mL every 4–5 days) affected *Stenotaphrum secundatum* (St. Augustine grass) over one month in Orange County, Southern California. Color was quantified using $a*:b*$ ratios, growth was tracked using grass area, and pigment composition was analyzed using plot profiles. We analyzed whole samples in the uncontrolled real-world environment, individual leaves in a controlled homemade imaging box, and extracted pigments before and after paper chromatography. Results were clustered using Gaussian finite mixture models, implemented by R package 'mclust'. Overall trends for grass coverage, $a*:b*$ ratios, and pigment composition were consistent with real-world observations. Cluster analyses were consistent across image types, identified an ideal watering range (600–700 mL), and differentiated between underwatered and overwatered grass. Our hypothesis was supported. Our method can be applied in automated irrigation systems or apps, providing grass WUE assessment for regular consumer use.

INTRODUCTION

Lawns, parks, golf courses, and school fields are common fixtures of the modern residential landscape. The prevalence of green spaces makes distribution of limited municipal water supplies a challenge (1). Overwatering and underwatering are common issues with consequences such as NO_3-N groundwater contamination, soil leaching, sunken turfgrass, damaged hardscapes, and stagnant water that may serve as reservoirs of infectious agents (2, 3). In fact, landscape watering accounts for the highest percentage of household water usage at 30–65% nationally (4). Homeowners use 30–70% of their water outdoors, and it is estimated that 50% of this water goes to waste due to evaporation, runoff, or overwatering (5). Moreover, residential landscapes are often given more water compared to the amount allocated towards ecosystem services (1). The evolving aridification issue has compounded watering challenges and led some cities to reduce nonfunctional turf or prioritize certain plants to reduce overall watering (6, 7).

Current water management and conservation strategies have not yielded a widely accessible tool to assess water use efficiency (WUE). Applicable methods include alternate sprinkler designs and smart irrigation (1). Weather-, sensor-, and schedule-guided irrigation are the most common strategies used to assess WUE (4). However, use of these technologies is limited to proactive consumers, price-sensitive environmentalists, content retirees, and high-end professionals, and thus is not widely accessible (8). Computational modeling and simulations have been used to develop better irrigation schemes and to test and optimize water management practices, but these are primarily relevant to policymaking and resource distribution, not the average person (4). Finally, existing water conservation apps track or estimate water usage without assessing lawn quality and WUE; those that generate suggested irrigation schedules are used primarily by the agriculture industry, not homeowners and communities (9). Thus, existing approaches are inaccessible or indirect to the public.

We aimed to address this issue by developing a nonbiased, quantitative method for WUE assessment. We primarily investigated grass color and growth because these are the most visible, direct indicators of lawn quality and WUE for the public. WUE is defined as the amount of carbon assimilated as biomass per unit of water consumed by the plant; it is a measurement of plant growth (10). Thus, grass growth is a direct indicator of WUE. Changes in grass color mark the stages of drought stress: lawns turn bluish-gray at the first stage, patchy yellow at the second stage, greenish-brown at the pre-dormant stage, and completely brown at the dormant

stage (11). Overwatering leads to thatch, fungal growth, weeds, and waterlogged grass, which all impact grass color (12). The balance of green and yellow color in a lawn impacts visual assessment of grass quality. These colors are the result of pigments involved in photosynthesis. Green color is due to chlorophyll *a* and chlorophyll *b*, which absorb light in the blue-violet and red-blue ranges of the visible spectrum, respectively, and reflect green wavelengths (13). Yellow color is due to carotenoids such as xanthophylls and β-carotene, which absorb light in the blue and blue-green ranges, respectively, and reflect yellow and orange wavelengths, respectively (14). Water stress directly impacts pigment levels by significantly decreasing chlorophyll *a* and *b* levels while significantly increasing carotenoid levels (15, 16). This leads to a decrease in green color and an increase in yellow color with decreasing WUE. Therefore, tracking grass color and growth allowed us to visualize and quantify the progression of grass quality and health depending on WUE.

Our method combines accessible smartphone imaging of grass samples with ImageJ CIELAB image analysis. ImageJ is an open-source, Java-based software for image processing and analysis that was developed by the National Institutes of Health (NIH) and is extensively used across scientific disciplines (17, 18). The principle behind our method's grass color analysis is the conversion of smartphone images from the RGB color space to the CIELAB color space using ImageJ software.

A color space is a tool used to visualize and quantify colors on a coordinate system, forming a three-dimensional object with all color combinations in that color space (19). All color spaces utilize the principles of color unmixing: the mathematical representation of digital color through fractions of pure color components in color spaces. RGB is the most common color space used by digital images and contains three dependent component axes: R (red), G (green), and B (blue) **(Figure 1a)**. Thus, the effects of varying brightness and lighting factors of uncontrolled, real-world imaging environments are inseparable from digital color perception. In contrast, CIELAB is a perceptually uniform color space that attempts to approximate human vision and unmixes brightness and lighting onto an independent *L** (lightness) axis (19). CIELAB also unmixes digital color onto two dependent component axes: *a** (unmixes the green to red vector) and *b** (unmixes the blue to yellow vector) **(Figure 1b)**. The pure components in CIELAB are, therefore, the *L*, *a**, and *b** vectors.

We wanted to determine whether combining CIELAB digital color unmixing with ImageJ analysis is an effective and accurate method for assessing grass WUE. We hypothesized that WUE can be accurately determined from grass color and growth. We predicted that CIELAB color unmixing would effectively analyze grass color and growth under the various lighting conditions of samples imaged in the real-world environment by separating lighting from color. ImageJ provides tools for measuring area, which can be used to track grass coverage and other morphological parameters as additional indicators of water stress (17). We first tested if CIELAB effectively reduces lighting factors of the real world to analyze smartphone images of grass. We then tested if the digital color unmixing of ImageJ CIELAB analysis is consistent with the physical pigment unmixing of paper chromatography.

Our results showed that ImageJ CIELAB analysis effectively quantified and tracked grass color and growth over time. The analysis differentiated between underwatered,
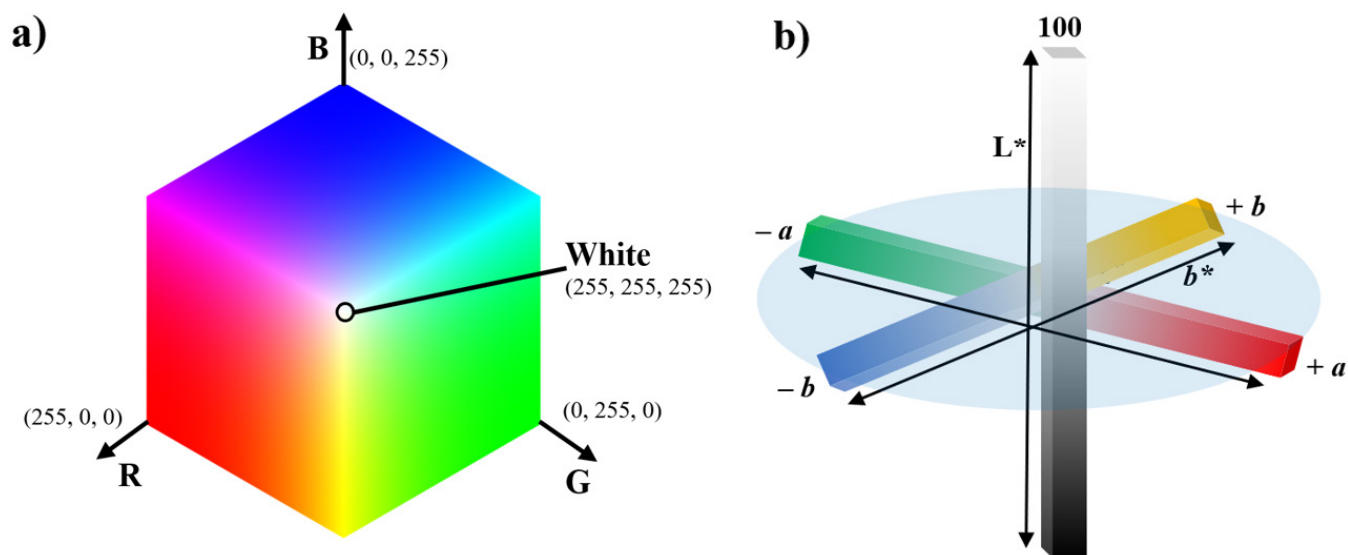
Figure 1. Comparison of RGB color space and CIELAB color space. (a) RGB has three dependent color axes, while **(b)** CIELAB has an independent *L** axis for lighting and two dependent color axes. From negative to positive, the *a** axis goes from green to red and the *b** axis goes from blue to yellow. The RGB image is modified from Wikipedia under a Creative Commons license, and the CIELAB image is an original image created in Microsoft PowerPoint.

ideal, and overwatered grass samples to determine an ideal watering range for WUE assessment. Our experiments indicated that CIELAB can effectively minimize lighting factors of uncontrolled, real-world environments and that the digital unmixing of CIELAB analysis is consistent with the physical unmixing of paper chromatography. Thus, we validated that smartphone imaging combined with ImageJ CIELAB analysis can effectively estimate grass WUE. Our results and methodology may serve as reference or inspiration for other researchers looking to develop the use of smartphone imaging and color space analysis to assess plants and environmental factors. Our study also has the potential to be expanded into practical applications for public and consumer use.

RESULTS

We analyzed the effects of 9 different watering levels (100–900 mL) on grass color and growth of *Stenotaphrum secundatum* (St. Augustine grass) samples over 1 month (July 2020) in Orange County, Southern California (33° 43' 03'' N, -117° 49' 52" W) using smartphone imaging and ImageJ CIELAB analysis. We watered each sample with a designated amount of water (100–900 mL for levels 1–9, respectively) every 4–5 days and imaged every 8–10 days.

We analyzed three types of smartphone images: whole samples in an uncontrolled real-word environment, individual leaves in a controlled environment of a homemade imaging box, and extracted pigments before and after separation by paper chromatography. Whole samples in the uncontrolled real-world environment represent the most direct assessment and mimic human perception. We used individual leaves imaged in the controlled imaging box to test if ImageJ CIELAB analysis effectively reduces lighting factors of the real world to analyze grass color. Extracted pigments before and after separation compared the digital unmixing of CIELAB analysis with the physical unmixing of paper chromatography.

We imaged all 9 whole samples 5 times each and imaged 3 leaves from each sample 4 times each, for a total of 45 whole samples and 108 individual leaves imaged. We ran one paper chromatography strip per watering level on the last imaging day for a total of 9 unseparated pigment images and nine separated pigment images. We used samples from the first imaging day as the controls to compare how grass color and growth changed over time with different watering levels. We clustered the differences between the last imaging day and the first imaging day for grass area and *a*:*b** ratios using Gaussian finite mixture models, implemented by R package 'mclust' (20).

Whole sample analysis

There was a visible loss of green color and coverage in levels 1–5 over 1 month in the raw whole sample images, while there was no loss of green color or coverage in levels 6–9 **(Figure 2a)**. Coverage refers to the percentage of the planter soil surface covered with grass when viewed from above. ImageJ analysis matched these observations. All

samples showed an initial increase in grass area, but levels 1–4 (cluster 1) decreased in coverage after late July to 49.51%, 49.91%, 51.72%, and 66.18%, respectively. Only levels 5–9 (cluster 2) maintained high coverage at 88.64%, 88.98%, 99.62%, 99.68%, and 100.29%, respectively **(Figure 2b)**. The whole sample grass area coverage trend reflected the decrease in grass area in lower levels and the maintenance of grass area in higher levels.

The color of levels 1–6 (cluster 1) increased in *a*:*b** ratios over time, while levels 7–9 (cluster 2) maintained more negative *a*:*b** ratios **(Figure 2c)**. Negative *a** values and positive *b** values are indicators of green and yellow intensity, respectively, so more negative *a*:*b** ratios indicate greener grass color. Thus, the increasing *a*:*b** ratios in the lower watering levels reflected the visible loss of green color, while the maintained *a*:*b** ratios in the higher levels reflected maintenance of grass color.

Individual leaf analysis

There was a visible decrease in green color in levels 1–4 and a maintenance of green color in levels 5–9 in the raw individual leaf images **(Figure 3a)**. The *a*:*b** ratios of levels 1–5 (cluster 1) increased over time, while the *a*:*b** ratios of levels 6–9 (cluster 2) consistently stayed in a negative initial range (-0.9, -0.7) **(Figure 3b)**. The *a*:*b** values of the individual leaf analysis were consistent with those of the whole sample analysis. This consistency indicates that CIELAB digital unmixing effectively removes lighting noise of uncontrolled real-world imaging environments to analyze grass color.

Pigment composition

Samples with higher watering levels had visibly greater pigment density and intensity before and after separation in the raw chromatography images **(Figure 4a)**. For unseparated pigments, levels 5–9 (cluster 2) had more negative *a*:*b** ratios in the range (-0.6, -0.4) compared to the *a*:*b** ratios of levels 1–4 (cluster 1) in the range (-0.4, -0.3) **(Figure 4b)**. The more negative *a*:*b** ratios of levels 5–9 reflected higher green pigment intensity compared to lower levels.

For separated pigments, levels 6–9 (cluster 2) had more negative *G* values and more positive *Y* values compared to levels 1–5 (cluster 1). *G* values decreased from -27.132 (level 1) to -224.844 (level 9), while *Y* values increased from 70.216 (level 1) to 241.960 (level 9) **(Figure 4c)**. The more negative *G* values and more positive *Y* values reflected higher overall pigment intensity in the higher levels. The consistent clustering results between unseparated and separated pigments showed that digital CIELAB unmixing is consistent with the physical unmixing of chromatography. These trends also reflected higher pigment production in levels 6–9 compared to levels 1–5. Matching plot profile trajectories showed that pigment composition remained consistent across all nine watering levels.

Clustering analysis

We analyzed data collected from the nine watering levels for all seven metrics using mclust Gaussian mixture modeling. For each metric, we calculated the difference between the first imaging day and the last imaging day for each watering level. We grouped the nine differences into two clusters and compared the means of the clusters using two-tailed two-sample t-tests. Across all seven metrics, levels 1–4 were classified into cluster 1 (underwatered levels), levels 7–9 were in cluster 2 (ideal and overwatered levels), and levels 5 and 6 varied. Cluster 1 means were significantly different from cluster 2 means, as shown by p-values < 0.05 **(Table 1)**.

Our clustering results revealed additional observations when analyzed together. While whole sample $a*:b*$ ratios grouped levels 5 and 6 in underwatered cluster 1, whole sample coverage grouped both transition levels in ideal and overwatered cluster 2 **(Figure 2b–c)**. This reflects how water stress manifested as changes in grass color before grass area was affected, which matches our real-world observations **(Figure 2a)**. Consistent clustering results between the G and Y pigments and the $a*:b*$ ratios of the unseparated pigments shows that CIELAB digital unmixing is consistent with the physical unmixing of paper chromatography **(Figure 4b–c)**.

Data and observations indicated that level 6 was the critical watering point. From the clustering analysis, level 6 varied between cluster 1 and cluster 2 depending on the metric, making it a transitional level between underwatered levels and ideal levels. We observed that level 6 showed visible signs of water stress at the whole sample level, including curling and yellow leaves. Levels 7–9, meanwhile, had vibrant green color and high grass density. Thus, we identified that the ideal watering level was between levels 6 and 7, corresponding to an ideal watering range of 600–700 mL and an $a*:b*$ range of (-0.8, -0.7).

DISCUSSION

The consistency of our whole sample and individual leaf analyses, and their agreement with real-world observations, strongly indicates that ImageJ CIELAB analysis can effectively analyze grass color and connect $a*:b*$ values to WUE. ImageJ also analyzed grass area and pigment composition—additional indicators of grass quality and water stress. Digital CIELAB unmixing reflected the loss of green color in lower watering levels and the maintenance of green color in higher watering levels. ImageJ area analysis reflected decreasing grass coverage of lower watering levels and maintenance of grass coverage of higher watering levels, demonstrating the impact of watering level on grass growth (10). The $a*:b*$ values of the unseparated pigments and the G and Y values of the separated pigments both indicated that our method can effectively analyze pigment composition.

Overall, our experiment results were consistent across all three image types and all seven analyses. Using our method, we found that grass color, area, and pigment analysis reflected water levels and WUE. Thus, our hypothesis was supported. The consistency between the $a*:b*$ ratios of whole samples and individual leaves suggested that CIELAB analysis effectively reduced lighting factors of the real-world environment to analyze grass color. Additionally, the consistency between unseparated and separated pigment analyses indicated that digital unmixing was consistent with physical unmixing.

We observed differences in grass color and growth among different watering levels in the field. To mathematically define this observation, we used clustering to group watering levels based on water use efficiency, as analyzed through our seven dependent variables. Since we assume that the data is normally distributed, we believe the parametric mclust method serves as an effective way of analyzing the data without prior knowledge of the number of clusters.

We identified an ideal watering range of 600–700 mL, which scales to approximately 0.235 gallons of water per square foot of St. Augustine grass for a circular sample with a 1 ft radius. This is less than the currently suggested 0.623 gallons of water per square foot for the average lawn (21). Our proposed ideal watering range consistently falls in the lower end of cluster 2, representing the least amount of water that still preserves grass color and growth. We used

Table 1. Summary of all seven cluster analyses.

Dependent Variable	Cluster 1 Mean	Cluster 1 Levels	Cluster 2 Mean	Cluster 2 Levels	p-value
Whole Sample Coverage Difference	13.185%	1–4	54.262%	5–9	0.00005197
Whole Sample $a*:b*$ Difference	0.431	1–6	0.016	7–9	0.0124
Individual Leaves $a*:b*$ Difference	0.385	1–5	0.024	6–9	0.0289
Unseparated Pigments $a*:b*$ Value	-0.360	1–4	-0.496	5–9	0.00245
Separated Pigments G Value	-40.758	1–5	-173.500	6–9	0.00182
Separated Pigments Y Value	92.197	1–5	278.980	6–9	0.000111

NOTE: *The means of the two clusters for each metric were significantly different (p-value < 0.05). Levels 1–4 were consistently in cluster 1 (underwatered levels), levels 7–9 were consistently in cluster 2 (ideal and overwatered levels), and levels 5 and 6 varied (transition levels). Overall, clustering results were consistent.*
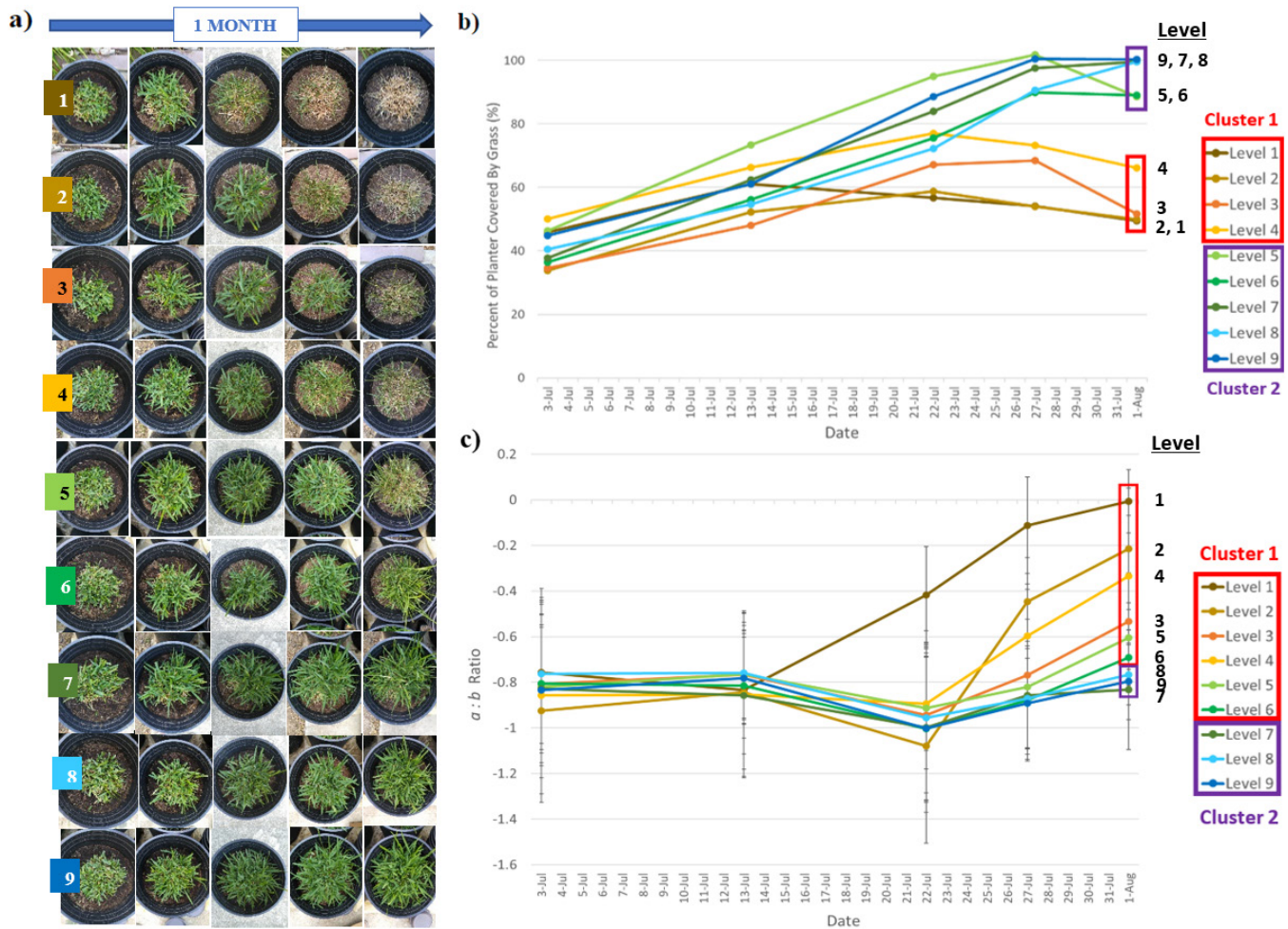
Figure 2. Grass color and growth in whole samples over one month of graded watering. (a) Raw whole sample images reflected macro changes in grass color and growth over one month of graded watering. **(b)** Grass coverage over one month of graded watering levels showed a decrease in coverage in levels 1–4 after July 21 and a maintenance of coverage in levels 5–9. **(c)** Whole sample $a*:b*$ ratios over one month of graded watering showed increasing $a*:b*$ ratios in levels 1–6 and consistently more negative $a*:b*$ ratios in levels 7–9. The error bars represent standard deviation.

the whole samples as the primary determinant of the ideal watering range and $a*:b*$ range because they provide the most practical, direct assessment of grass WUE.

Our results are consistent with similar studies. In two previous studies, CIELAB effectively removed camera noise and was determined to be the ideal color space for assessing plant disease and leaf area (22, 23). Another study found that CIELAB had the highest sensitivity and specificity among a panel of color spaces (RGB, HSV, CIELAB, YCbCr) and studied potential applications of CIELAB technology in smart farming (24). Another study used the RGB to CIELAB conversion in a cascaded algorithm to successfully identify plant diseases (25). These studies all identified CIELAB as an ideal color space for plant image analysis and demonstrated that the RGB to CIELAB image analysis method can be used to accurately assess plant health.

In conclusion, our results demonstrated the effectiveness and potential of an accessible original approach to water conservation. Our work effectively combines smartphone

imaging with ImageJ CIELAB analysis to analyze grass color, growth, and pigment composition to determine ideal watering ranges. Our study is consistent with previous studies using CIELAB analysis to analyze plants, but it is the first to use CIELAB unmixing to assess the effects of watering on grass color and growth. We also showed that digital CIELAB unmixing is consistent with the physical unmixing of paper chromatography, thereby validating the principles of color space conversion using an accessible lab technique.

One limitation of our study is that we could have extended our experiments for a longer time to check if trends in grass color and growth continued. A longer study would have allowed us to determine whether signs of overwatering damage, which were appearing by the end of the experiment period, could be reflected in $a*:b*$ ratio and coverage. Distinguishing between the yellowing and browning of sunken roots in severely overwatered grass and the yellowing and browning of underwatered grass also needs to be further developed. Finally, ImageJ CIELAB analysis was time-consuming when
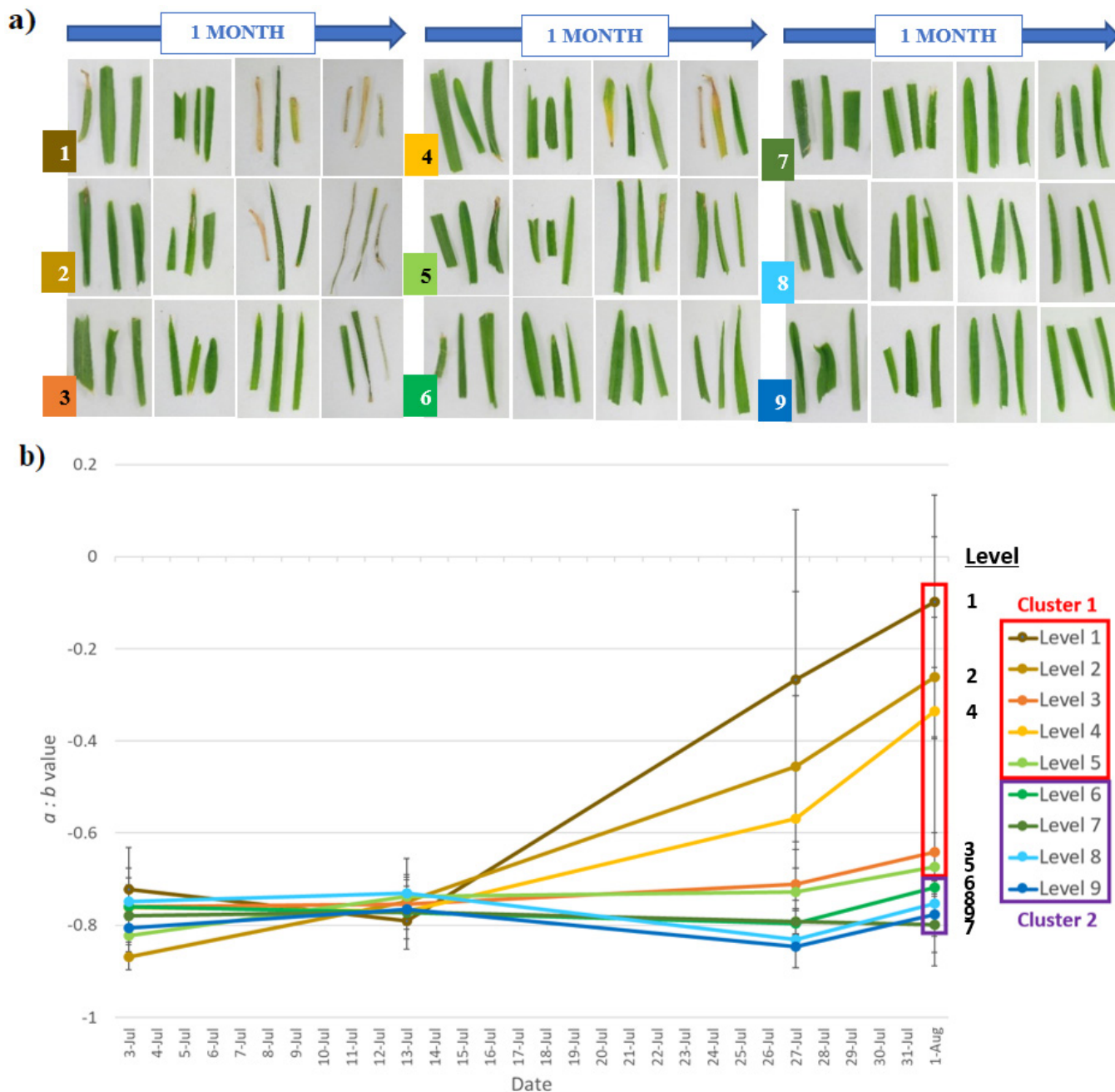
Figure 3. Grass color and growth in individual leaves over one month of graded watering. (a) Raw individual leaf images reflected changes in grass color in the controlled imaging box environment. **(b)** The *a*:b** ratios of individual leaves over one month of graded watering showed increasing *a*:b** ratios in levels 1–5 and more negative *a*:b** ratios in levels 6–9. The error bars represent standard deviation.

completed manually for each image, and human bias could have impacted ROI selection, although the effect of bias on results was likely insignificant because we analyzed average values. An immediate next step would be to write an algorithm for the digital unmixing analysis process.

In addition, grass color is determined by many factors besides watering, including temperature, climate, soil type, fertilization, and grass type (26). Our study focused on the effects of watering, so additional studies need to be conducted to analyze the effects of geographic location,

environment, soil composition, nutrient levels, and pH into the WUE assessment. A database of standard *a*:b** ranges based on grass type and these additional factors would need to be constructed through additional experiments and simulations. Finally, having one grass sample per watering level resulted in a small sample size. Replicates would have presented a more accurate assessment of which samples were underwatered or overwatered.

Future experiments would also expand our method's potential for practical applications. An immediate application
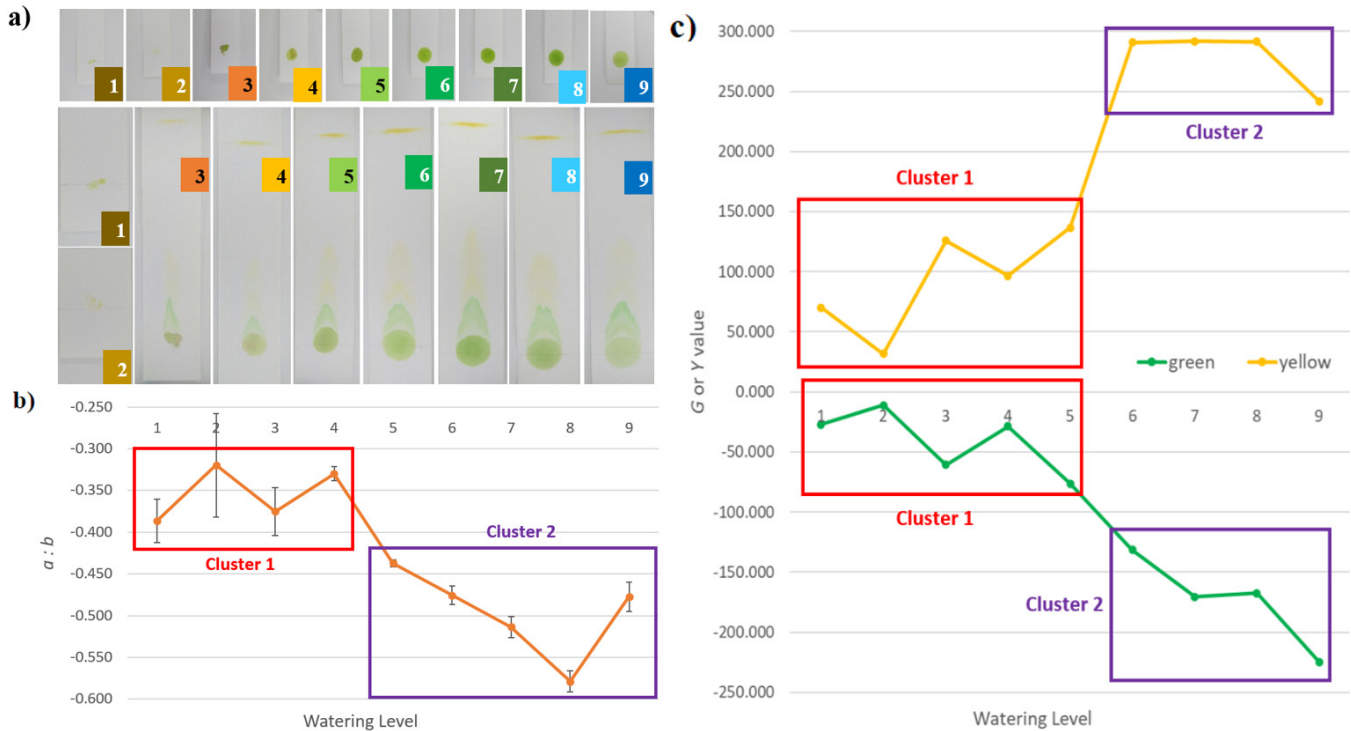
Figure 4. Pigment composition analysis using paper pigment chromatography. (a) Raw unseparated pigment images and separated pigment images reflected greater pigment density and intensity with higher levels of watering. **(b)** The *a*:*b** ratios of unseparated pigments showed more negative *a*:*b** ratios in levels 5–9 compared to levels 1–4. We used ImageJ to calculate the standard deviations for *a** and *b** values in each image based on the *a** and *b** values of all pixels in the selected region of interest. **(c)** G and Y pigment values of separated pigments reflected the higher pigment production and overall pigment intensity of levels 6–9 compared to levels 1–5.

would be an app that provides instant grass WUE assessment for consumer use. Ideally, users would photograph an area of grass and the app would calculate the *a** and *b** values, compare it to a standard set of *a** and *b** values determined by further experimentation, and mark the sample as underwatered, overwatered, or ideally watered. Additional applications include integrating our method into automated gardening systems to track and preserve grass WUE and the health of other plant species by linking watering and lighting apparatus (24). Scaling our method to satellite or drone imaging would enable application in residential parks, golf courses, and cities, or aid in socioeconomic and horticulture studies. Green space distribution, for example, is an indicator of economic equity and urban ecological environment with the potential to decrease health inequality between socioeconomic and sociodemographic groups (27-29). Urban green space is directly connected to urban horticulture—one solution to the growing food insecurity issue—and is currently studied using spatiotemporal simulations and analysis of open-source datasets (27, 30-31). Applying our method to large-scale images could provide direct analysis for the study of urban green space and horticulture development and impact.

Our study validated the reliability of CIELAB image analysis independent of chromatography and the imaging box. For public use, CIELAB image analysis would be used directly,

although calibration of the method to real-world systems would be necessary in application development processes. Such applications would make grass WUE assessment more accessible to the public and better equip homeowners, industries, and community leaders for water conservation.

MATERIALS AND METHODS
Imaging box construction and calibration

The imaging box was constructed from two cardboard boxes. The first was a 40.5 cm x 30 cm x 28 cm cardboard box with a 31 cm x 21.5 cm opening cut out of the side facing the user. The second was a 45 cm x 33 cm x 10 cm box with a hole of radius 13 cm cut out of the top face. The second was inserted horizontally into the opening of the first with the hole facing upwards **(Figure 5a)**. A sheet of blank white printer paper was used to cover the inside bottom of the first box directly below the hole, and four identical LED side-bar flashlights were secured on four 4 cm x 10 cm x 15 cm index card platforms oriented against each other and the sides of the box to form the 10 cm x 10 cm imaging space. We applied the photography principle of soft-boxing—when light is released through a layer of diffusion to minimize shadows and scatter light more evenly across an imaging space—to our light sources. Each flashlight was soft-boxed by taping two KIMTECH™ wipers over the light source **(Figure 5b)**. A plastic clipboard was used to hold a ZenFone 3 Android
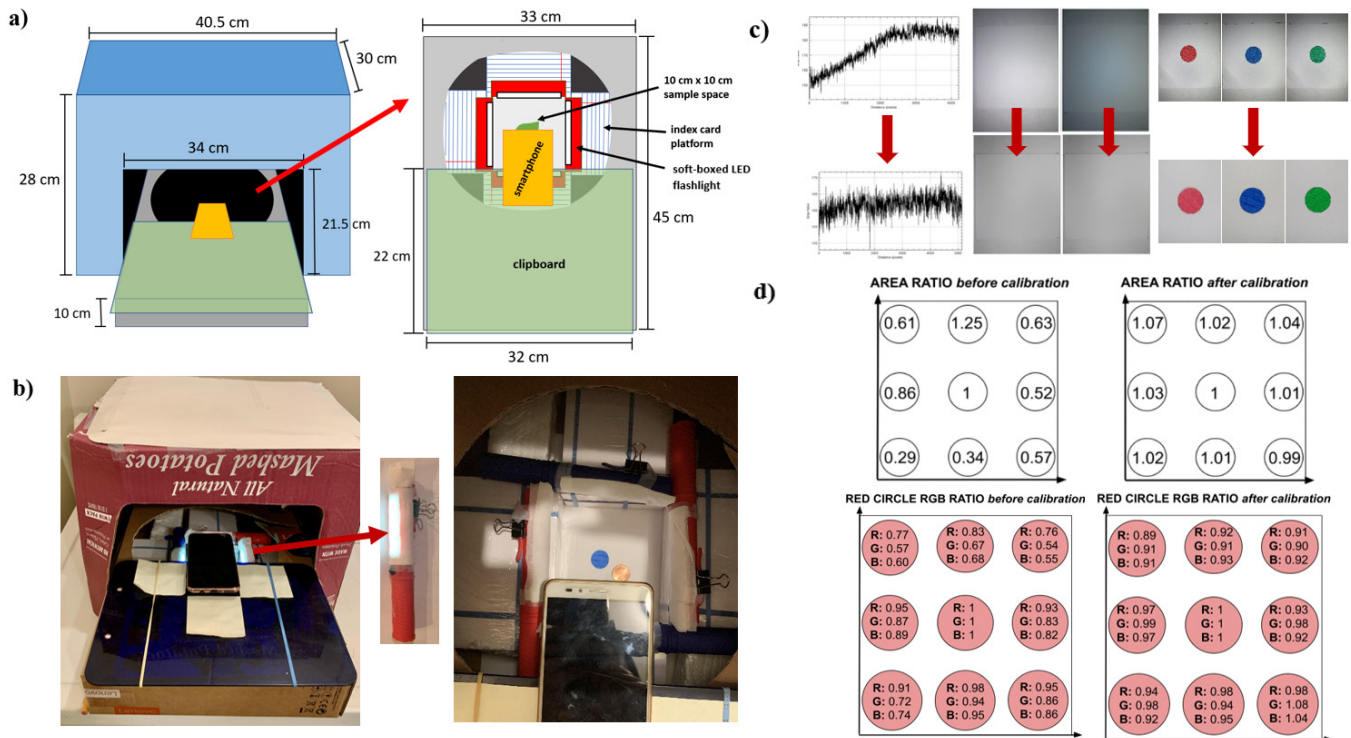
Figure 5. Imaging box construction and calibration procedures. (a) Schematic of the homemade imaging box from the exterior (left) and the imaging space (right). Smartphone imaging was done from above the sample space, which was illuminated with four soft-boxed LED flashlights. **(b)** The imaging box from the exterior (left), a soft-boxed LED flashlight (center), and the imaging space (right). **(c)** Imaging before and after calibration. Plot profiles (left) were used to track lighting calibration, with "flattening" of the plot profile reflecting more uniform illumination. Apple vs. Android smartphone and digital flash vs. no digital flash (center) were tested. Astigmatism was handled using 1.7x digital zoom (right), which discarded the border regions of inconsistency. **(d)** Example reference plots used to visualize and track calibration across area, perimeter, aspect ratio, center of mass, and RGB color. The center region was used as a reference and set to one for all parameters. Calibrated images yielded ratios closer to one for the other eight regions.

smartphone above the imaging space.

Calibration focused on addressing chromatic aberrations and astigmatism by creating uniform illumination and testing different configurations. Illumination was analyzed using plot profiles. Astigmatism was reduced using 1.7x digital zoom to discard border regions of astigmatism **(Figure 5c)**. In our calibration imaging trials, we imaged red, green, and blue paper circles across nine regions in the imaging space and analyzed area, perimeter, aspect ratio, center of mass, and RGB color. Reference plots with the center region set to one for all calibration parameters were used to visualize and track the calibration process. The optimized configuration was chosen because it resulted in reference ratios closest to one **(Figure 5d)**.
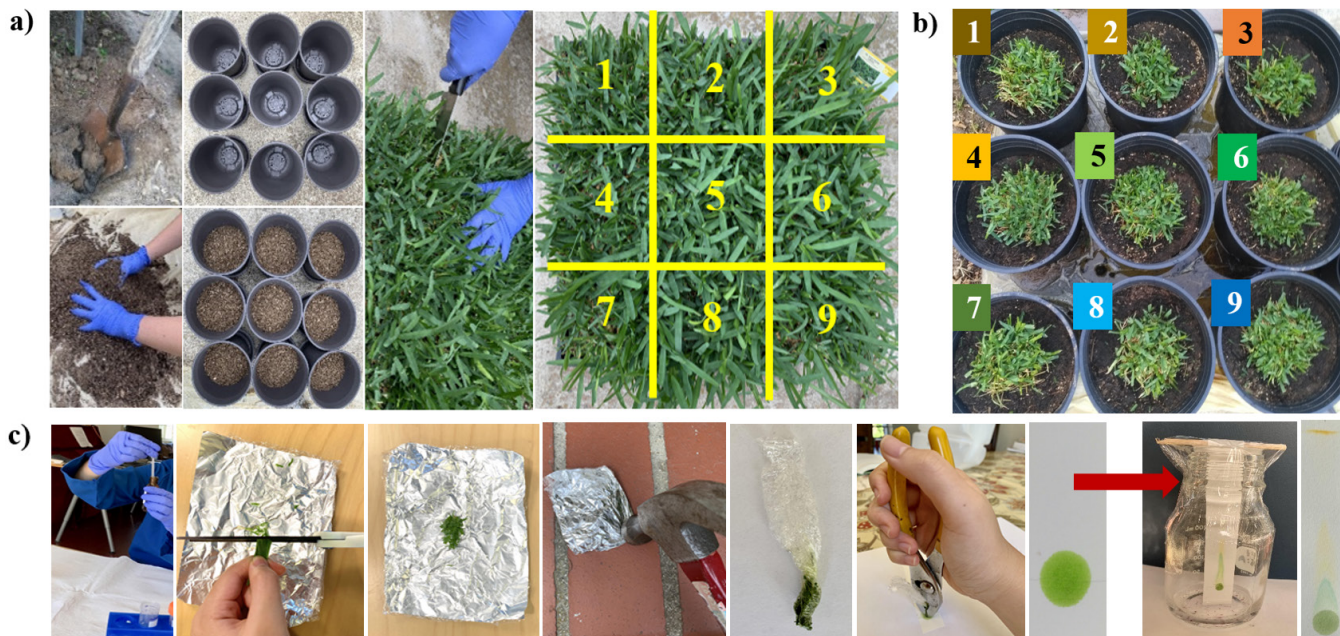
Grass sample preparation and watering

A soil mixture was prepared by hand-mixing 10 parts backyard soil with 1-part Sta-green lawn starter. Nine 1 L plastic planters were filled to the two-thirds mark with soil mixture. A 42 cm x 42 cm St. Augustine seedling plug was cut using a kitchen cleaver into nine 14 cm x 14 cm squares **(Figure 6a)**. Each sample was trimmed into a circular shape using gardening shears, then potted into a plastic planter with

soil mixture. The planters were placed in an area that received around six hours of sunlight daily. The watering scheme was determined by adding water in 100 mL increments to a sample until water began passing out of the bottom of the planter, which occurred around 500 mL. This amount of water was set as the fully watered midpoint level. To include underwatering and overwatering, the graded watering scheme was expanded to 100–900 mL **(Figure 6b)**. For the first 10 days, all samples were given 600 mL twice per week to stabilize the seedlings in their new environment. Then, each pot was watered with its designated amount every 5 days from July 3 to July 17, then every 4 days from July 18 to August 1 due to rising daily temperatures. Watering was conducted by adding 100 mL increments of water evenly across the grass samples using a 250 mL measuring cup.

Sample imaging

We imaged and compared three distinct types of Android smartphone images. First, on every other watering day, each whole sample was imaged from 25–30 cm above the sample. Next, on every other imaging day, three individual leaves were selected from three designated, consistent regions spread across each whole sample and imaged in

Figure 6. Grass sample preparation procedures. (a) Grass sample preparation using a soil mixture and St. Augustine seedling plugs. **(b)** Potted and stabilized grass samples on the first imaging day, labeled with the nine watering levels. Levels 1–9 were watered with 100–900 mL, respectively, every 5 days from July 3 to July 17, 2020, and every 4 days from July 18 to August 1, 2020. **(c)** Paper chromatography solvent preparation, pigment extraction procedures, and paper chromatography apparatus.

the controlled environment of the homemade imaging box. Individual leaf imaging was performed immediately after leaf collection across all imaging days. Finally, extracted pigments before and after separation by paper chromatography were imaged in the imaging box.

Pigment extraction and paper chromatography

Thirty mL of 9:1 petroleum ether (Home Science Materials) to acetone solvent (Target) was prepared in a 250 mL flask, which was immediately sealed with plastic wrap **(Figure 6b)**.

For each watering level, the three individual leaves from each whole sample were aligned over a 12 cm x 12 cm aluminum foil piece covered with plastic wrap and shredded with scissors. The foil was folded in half twice with the shredded leaves concentrated in the innermost corner. If the leaves were visibly dry, 1 mL of solvent was added. The corner was smashed gently with a hammer, the foil was stripped away, and the plastic wrap was twisted to form a snub with the smashed grass at one end. A toothpick was used to break a small hole at the tip of the snub, and a needle nose plier
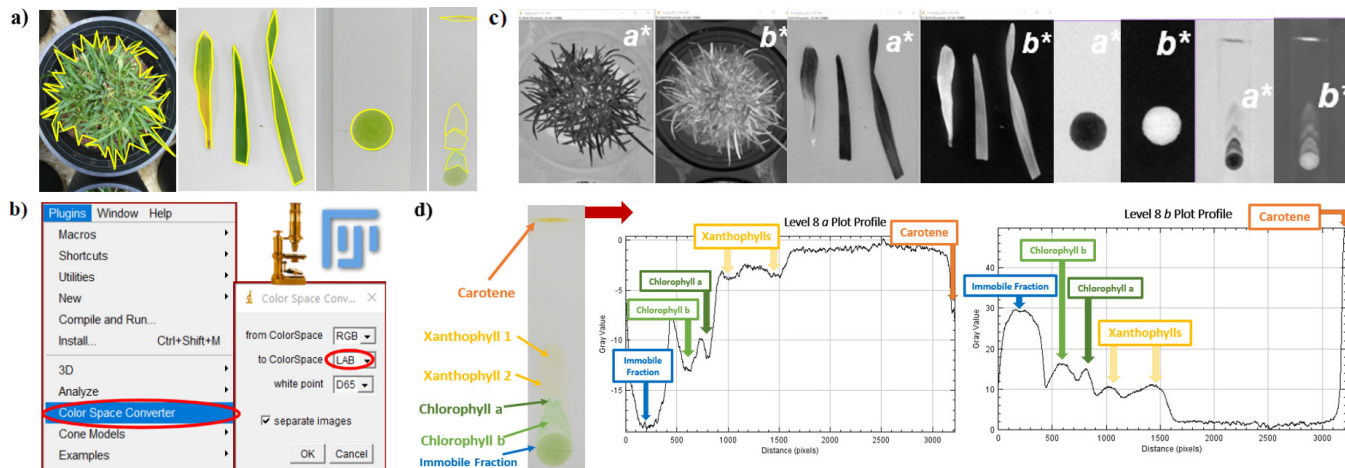
Figure 7. ImageJ CIELAB and plot profile analysis procedures. (a) Region of interest (ROI) selection in whole samples, individual leaves, and extracted pigments. **(b)** Color space conversion from RGB to CIELAB digitally unmixes the smartphone images onto the L*, a*, and b* axes. **(c)** Examples of the digitally unmixed a* and b* channel images for all three image types. **(d)** Labeled pigment separation and corresponding example a* and b* plot profiles. Dips in the a* plot profile and peaks in the b* plot profile correspond to different pigments.

was used to squeeze two drops of pigment onto the loading line of a paper chromatography strip. The sample was imaged in the imaging box. Then, each chromatography strip was suspended using a chopstick over a flask and was run for 6–7 minutes until pigments were visibly separated. Immediately after running, the sample was imaged in the imaging box.

ImageJ CIELAB analysis

Each image was opened in ImageJ, and the region of interest (ROI) was chosen and saved to the ROI Manager using the selection tools **(Figure 7a)**. For individual leaves, each leaf was an independent ROI. For separated pigments, an overall ROI was selected by dragging the thickened line selection tool from the bottom of chlorophyll *b* through the top of carotene. Each pigment was also selected as an independent ROI. Each image was converted to CIELAB using the Color Space Converter plugin with separate channels **(Figure 7b)**. The selected ROIs were applied to the unmixed images. Whole sample grass areas and *a*:*b** values were obtained using the measurement tool and histogram tool, respectively **(Figure 7c)**.

Plot profiles were used to analyze separated pigment images. The overall ROI plot profile was used to visualize pigment separation and composition. We assumed that green pigments contributed to green color and yellow pigments contributed to yellow color. Thus, individual pigment values were calculated by multiplying individual pigment ROI areas by mean *a** (green) values for chlorophyll *a* and chlorophyll *b* (green pigments) and by mean *b** (yellow) values for xanthophylls and carotene (yellow pigments) (13, 14) **(Figure 7d)**. *G* values were the sum of the chlorophyll pigment values, and *Y* values were the sum of the xanthophyll and carotene pigment values. *G* and *Y* values were only used for paper chromatography analysis to factor in smearing and varying degrees of pigment separation. We analyzed green and yellow color separately in the separated pigments to directly compare physical unmixing with digital unmixing.

Statistical analysis

Standard deviations for *a*:*b** ratios were calculated using the *a** and *b** values for each image. For whole samples, ImageJ calculated the standard deviations for *a** and *b** values in each image based on the *a** and *b** values of all pixels in the selected region of interest. We used the Taylor Series Methods with the assumption that covariance of a* and b* is equal to 0 to calculate standard deviations (32). For individual leaves, average *a*:*b** ratios and standard deviations were calculated using the three *a*:*b** ratios of the individual leaves of each watering level on each imaging day.

Differences in grass area, whole sample *a*:*b** ratios, and individual leaf *a*:*b** ratios on the last imaging day (August 1) and the first imaging day (July 3) were analyzed using Gaussian finite mixture models, implemented by R package 'mclust' (20). The analysis was used to determine the clusters of effects by nine watering levels (100–900 mL) based on

measurements that reflected changes in grass area and color. Watering levels with similar experimental measurements were placed in the same cluster, whereas watering levels in different clusters had distinct effects on grass area and color. Unseparated pigment *a*:*b** values, representing digital unmixing, and green and yellow pigment values and ratios, representing physical unmixing, were used for clustering analysis and further comparison using two-tailed two-sample t-tests.

REFERENCES

1. St. Hilaire, R., *et al*. "Efficient Water Use in Residential Urban Landscapes." *HortScience*, vol. 43 no. 7, December 2008, pp. 2081–2092. doi: 10.21273/HORTSCI.43.7.2081
2. Morton, T. G., *et al*. "Influence of Overwatering and Fertilization on Nitrogen Losses from Home Lawns." *Journal of Environmental Quality*, vol. 17, no. 1, 01 January 1988, pp. 124–130. doi: 10.2134/jeq1988.00472425001700010019x
3. Wallace, V., and A. Siegel-Miles. "Best Management Practices: Turfgrass Irrigation." University of Connecticut, College of Agriculture, Health, and Natural Resources. May 2017. www.aquarionwater.com/docs/default-source/conservation/best-management-practices-turfgrass-irrigation.pdf?sfvrsn=1ac73012_7. Accessed 5 June 2021.
4. Wolfe, J., III, J. Jeong, and K. Paulk. "Simulating urban irrigation practices to optimize outdoor municipal water use." *American Geophysical Union Fall Meeting Abstracts*, H33R-2305, December 2018.
5. "When it's Hot." *United States Environmental Protection Agency*. www.epa.gov/watersense/when-its-hot. Accessed 13 June 2021.
6. Burdick, Alan. "Where the Grass is Greener, Except When It's 'Nonfunctional Turf,'" *The New York Times*, 11 June 2021. www.nytimes.com/2021/06/11/science/drought-las-vegas-grass-mars.html. Accessed 13 June 2021.
7. Tabin, Sara. "Utah County to reduce park water usage by an average of 40%," *The Salt Lake Tribune*, 9 June 2021.

www.sltrib.com/news/2021/06/09/utah-county-reduce-park/. Accessed 13 June 2021.

8. Khachatryan, H., *et al*. "Who is interested in purchasing smart irrigation systems?" Institute of Food and Agricultural Sciences Extension, University of Florida. 2019. edis.ifas.ufl.edu/publication/FE1069. Accessed 20 March 2022.

9. "10 Useful Water Conservation Apps." *Seametrics*. www.seametrics.com/blog/water-conservation-apps/. Accessed 13 June 2021.

10. Hatfield, J. L., and C. Dold. "Water-Use Efficiency: Advances and Challenges in a Changing Climate." *Frontiers in Plant Science*, vol. 10, 19 February 2019. doi.org/10.3389/fpls.2019.00103

11. "Lawn Maintenance: The 4 Stages of Drought Stress." *Trugreen*. www.trugreen.com/lawn-care-101/learning-center/grass-basics/dig-deeper/4-stages-of-drought-stress#:~:text=During%20the%20first%20stage%20of,within%20a%20day%20or%20two. Accessed 20 March 2022.

12. "How to Spot Over-Watered Grass in Your Lawn." *Professional Irrigation Systems*. www.proirrigation.com/news-tips/signs-of-over-watering/. Accessed 20 March 2022.

13. Boundless General Microbiology at Boundless. "8.2B: Absorption of Light." *LibreTexts Biology*, 1 December 2020. bio.libretexts.org. Accessed 20 March 2022.

14. Galinato, M. G. I., *et al*. "Cation radicals of xanthophylls." *Photosynthesis Research*, vol. 94 no. 1, 19 July 2007, pp. 67–78. doi: 10.1007/s11120-007-9218-5

15. Hazrati, S., *et al*. "Effects of water stress and light intensity on chlorophyll fluorescence parameters and pigments of Aloe vera L." *Plant Physiology and Biochemistry*, vol. 106, September 2016, pp. 141–148. doi.org/10.1016/j.plaphy.2016.04.046

16. Mohammadkhani, N. and R. Heidari. "Effects of water stress on respiration, photosynthetic pigments and water content in two maize cultivars." *Pak J Biol Sci*, vol. 10 no. 22, 15 November 2007. doi: 10.3923/pjbs.2007.4022.4028

17. Schneider, Caroline A., W.S. Rasband, K. W. Eliceiri. "NIH Image to ImageJ: 25 years of Image Analysis." *Nature Methods*, vol. 9, no. 7, 28 June 2012, pp. 671–675. doi: 10.1038/nmeth.2089

18. Rueden, C.T., *et al*. "ImageJ2: ImageJ for the next generation of scientific image data." *BMC Bioinformatics*, vol. 18 no. 529, 29 November 2017. doi.org/10.1186/s12859-017-1934-z

19. "Color Management: Color Spaces." *Cambridge in Color*. www.cambridgeincolour.com/tutorials/color-spaces.htm. Accessed 10 June 2020.

20. Fraley C. and A. E. Raftery. "Model-based clustering, discriminant analysis and density estimation." *Journal of the American Statistical Association*, vol. 97 no. 458, 31 December 2011, pp. 611–631. doi: 10.1198/016214502760047131

21. "How to Calculate Lawn Irrigation Water Use and Costs." *Today's Homeowner*. todayshomeowner.com/calculating-lawn-irrigation-costs/. Accessed 25 June 2021.

22. Chaudhary, P. *et al*. "Color Transform Based Approach for Disease Spot Detection on Plant Leaf." *International Journal of Computer Science and Telecommunications*, vol. 3, no. 6, June 2012, pp. 65–69. www.ijcst.org/Volume3/Issue6/p12_3_6.pdf

23. Chaudhary, P. *et al*. "Fast and Accurate Method for Leaf Area Measurement." *International Journal of Computer Applications,* vol. 49, no. 9, July 2012, pp. 22–25. doi: 10.1.1.258.7607.

24. Loresco, P. J. M., I. C. Valenzuela, and E. P. Dadios. "Color Space Analysis Using KNN for Lettuce Crop Stages Identification in Smart Farm Setup." *TENCON 2018–2018 IEEE Region 10 Conference*, pp. 2040–2044. doi: 10.1109/TENCON.2018.8650209

25. Khan, Z. U. *et al*. "Automatic detection of plant diseases; utilizing an unsupervised cascaded design." *15th International Bhurban Conference on Applied Sciences and Technology (IBCAST)*, 2018, pp. 339–346. toc.proceedings.com/38706webtoc.pdf

26. Stichler, Charles. "Grass Growth and Development," Extension Agronomist, Texas A&M University. 2002. counties.agrilife.org/kerr/files/2011/09/grass-growth-and-development_3.pdf. Accessed 10 June 2020.

27. Li, F., et. al., "Spatiotemporal Simulation of Green Space by Considering Socioeconomic Impacts Based on A SD-CA Model." *Forests*, vol. 12 no. 2, 10 February 2021. doi.org/10.3390/f12020202

28. Wu, L., and S. K. Kim. "Does socioeconomic development lead to more equal distribution of green space? Evidence from Chinese cities." *Science of the Total Environment*, vol. 757, 25 February 2021. doi.org/10.1016/j.scitotenv.2020.143780

29. Kabisch, N. "The Influence of Socio-economic and Socio-demographic Factors in the Association Between Urban Green Space and Health." *Biodiversity and Health in the Face of Climate Change*, 12 June 2019, pp. 91–119. doi.org/10.1007/978-3-030-02318-8_5

30. Edmonson, J. L., *et al*. "The hidden potential of urban horticulture." *Nature Food*, vol. 1, 17 March 2020, pp. 155–159. doi.org/10.1038/s43016-020-0045-6

31. Solankey, S. S., *et al. Urban Horticulture: Necessity of the Future*. IntechOpen, 2020, pp. 169. doi: 10.5772/intechopen.82900

32. Wolter, Kirk M. "Taylor Series Methods." *Introduction to Variance Estimation*. New York: Springer. pp. 221–247, 1985. ISBN 0-387-96119-4.